J|A|C|S
ARTICLES

Published on Web 09/02/2010

Uranium Pyrophosphate/Methylenediphosphonate Polyoxometalate Cage Clusters

Jie Ling, Jie Qiu, Ginger E. Sigmon, Matthew Ward, Jennifer E. S. Szymanowski, and Peter C. Burns*

Department of Civil Engineering and Geological Sciences, University of Notre Dame, Notre Dame, Indiana 46556

Received June 2, 2010; E-mail: pburns@nd.edu

Abstract: Despite potential applications in advanced nuclear energy systems, nanoscale control of uranium materials is in its infancy. In its hexavalent state, U occurs as $(UO_2)^{2+}$ uranyl ions that are coordinated by various ligands to give square, pentagonal, or hexagonal bipyramids. Creation and design of nanostructured uranyl materials requires interruption of the tendency of uranyl bipyramids to share equatorial edges to form infinite sheets that occur in extended structures. Where a bidentate peroxide group bridges uranyl bipyramids, the configuration is inherently bent, fostering formation of cage clusters. Here the bent configurations of four- and five-membered rings of uranyl peroxide hexagonal bipyramids are bridged by pyrophosphate or methylenediphosphonate, creating eight chemically complex cage clusters with specific topologies. Chemical complexity in such clusters provides opportunities for the tuning of cage sizes, pore sizes, and properties such as aqueous solubility. Several of these are topological derivatives of simpler clusters that contain only uranyl bipyramids, whereas others exhibit new topologies.

Introduction

U(VI), like Np(V), Np(VI), Pu(V), and Pu(VI), usually occurs as a linear dioxo cation in solution and in the solid state.[1] Current research emphasizing the complex chemistry of actinyl ions, especially of the U(VI) $(UO_2)^{2+}$ uranyl ion, is providing unexpected results that are challenging our understanding of this normally unreactive functional group.[2,3] However, despite the tremendous importance of U(VI) in the nuclear energy cycle, opportunities for control of U(VI) chemistry at the nanoscale are largely undeveloped. Recognition of the potential importance of nanostructured actinyl materials in advanced nuclear energy cycles inspired the synthesis of uranyl selenate nanotubules[4] and cage clusters of uranyl peroxide polyhedra in 2005.[5] Studies have since shown that the self-assembly of uranyl isopolyhedra or heteropolyhedra into open and cage clusters containing as many as 60 U atoms occurs in aqueous solutions under ambient conditions.[3,5−8] Such clusters exhibit a fascinating range of topologies, including several examples of fullerenes with 20−60 uranyl polyhedra, with the latter topologically identical to C_{60} buckminsterfullerene.

The O atoms of the uranyl ion are strongly bonded to the central U(VI) cation of the dioxo cation, and they tend not to form strong interactions with additional cations. In most compounds uranyl ions are coordinated by four, five, or six ligands that are arranged at the equatorial vertexes of square, pentagonal, or hexagonal bipyramids. The O atoms of the uranyl ions occur at the apexes of these bipyramids. In solids, these uranyl bipyramids often share equatorial edges with either other uranyl bipyramids or a variety of oxyanions. As these linkages are through the equatorial positions of the bipyramids, infinite sheets are most often the result. Creation of nanoscale uranyl materials requires disrupting the tendency toward linkage of uranyl bipyramids into sheets. We reported that this may be accomplished using peroxide groups to bridge between uranyl ions located along shared equatorial edges of bipyramids.[7] Linkage of uranyl ions through peroxide groups was first found in the mineral studtite[9] and later in various clusters of uranyl peroxide polyhedra.[3,5−8] The U−(O_2)−U (uranyl−peroxide−uranyl) bridge is inherently bent[7] and encourages self-assembly of bipyramids into clusters rather than into infinite sheets.

Structural fragments built from uranyl bipyramids using peroxide bridges may induce curvature in cage clusters that contain other types of polyhedra. Here we report a family of eight uranyl peroxo pyrophosphate cage clusters where pyro-

(1) Morss, L. R.; Edelstein, N. M.; Fuger, J.; Katz, J. J. *The chemistry of the actinide and transactinide elements*; Springer: Dordrecht, 2006.
(2) Arnold, P. L.; Patel, D.; Wilson, C.; Love, J. B. *Nature* **2008**, *451*, 315. Boncella, J. M. *Nature* **2008**, *451*, 250. Burns, C. J. *Science* **2005**, *309*, 1823. Evans, W. J.; Kozimor, S. A.; Ziller, J. W. *Science* **2005**, *309*, 1835. Fox, A. R.; Bart, S. C.; Meyer, K.; Cummins, C. C. *Nature* **2008**, *455*, 341. Hayton, T. W.; Boncella, J. M.; Scott, B. L.; Palmer, P. D.; Batista, E. R.; Hay, P. J. *Science* **2005**, *310*, 1941. Summerscales, O. T.; Cloke, F. G. N.; Hitchcock, P. B.; Green, J. C.; Hazari, N. *Science* **2006**, *311*, 829.
(3) Burns, P. C.; Kubatko, K. A.; Sigmon, G.; Fryer, B. J.; Gagnon, J. E.; Antonio, M. R.; Soderholm, L. *Angew. Chem., Int. Ed.* **2005**, *44*, 2135.
(4) Krivovichev, S. V.; Kahlenberg, V.; Tananaev, I. G.; Kaindil, R.; Mersdorf, E.; Myasoedov, B. F. *J. Am. Chem. Soc.* **2005**, *127*, 1072.
(5) Sigmon, G. E.; Unruh, D. K.; Ling, J.; Weaver, B.; Ward, M.; Pressprich, L.; Simonetti, A.; Burns, P. C. *Angew. Chem., Int. Ed.* **2009**, *48*, 2737.
(6) Forbes, T. Z.; McAlpin, J. G.; Murphy, R.; Burns, P. C. *Angew. Chem., Int. Ed.* **2008**, *47*, 2824.
(7) Sigmon, G.; Ling, J.; Unruh, D. K.; Moore-Shay, L.; Ward, M.; Weaver, B.; Burns, P. C. *J. Am. Chem. Soc.* **2009**, *131*, 16648.
(8) Sigmon, G. E.; Weaver, B.; Kubatko, K. A.; Burns, P. C. *Inorg. Chem.* **2009**, *48*, 10907.
(9) Burns, P. C.; Hughes, K. A. *Am. Mineral.* **2003**, *88*, 1165. Hughes Kubatko, K.-A.; Helean, K. B.; Navrotsky, A.; Burns, P. C. *Science* **2003**, *302*, 1191.

Table 1. Additional Reactants Added to Synthesis Experiments

	$U_{18}Py_2PCP_6$	$U_{20}Py_{10}$	$U_{20}Py_{6a}$	$U_{20}Py_{6b}$	$U_{24}Py_{12}$	$U_{24}PCP_{12}$	$U_{26}Py_6$	$U_{26}Py_{11}$	$U_{32}Py_{16}$
$CH_2(PO_3H_2)_2$	0.1 mL of 0.2 M					0.3 mL of 0.1 M			
$K_4P_2O_7$	0.1 mL of 0.1 M	0.1 mL of 0.5 M	0.05 mL of 0.5 M	0.05 mL of 0.5 M			0.05 mL of 0.5 M	0.1 mL of 0.2 M	
$CH_3OHC(PO_3H_2)_2$		0.125 mL of 0.5 M							
$N(CH-COOH)_3$			0.1 mL of 0.1 M						
HOOC−COOH				0.1 mL of 0.5 M	0.1 mL of 0.5 M			0.1 mL of 0.5 M	0.2 mL of 0.5 M
$Na_4P_2O_7$					0.5 mL of 0.1 M				0.3 mL of 0.1 M
NaCl						0.2 mL of 0.1 M			
HOOC−CH=CH−COOH							0.1 mL of 0.5 M		
pH	7.3	8.7	10.3	9.3	7.2	6.7	10.4	10.3	5.3
pH range[a]	7.3−8.5	8.7−9.2	10.3−11.5	9.2−9.5	7.2−10.0	4.0−9.1	10.2−10.8	10.3	5.3

[a] The pH range given for each cluster is for all syntheses that resulted in the specific cluster.

phosphate units bridge between curved uranyl peroxide structural units. In two cases, methylenediphosphonate units are used in combination with, or replacing, the pyrophosphate units. Pyrophosphate and methylenediphosphonate were selected as promising ligands for creation of chemically complex nanostructured clusters containing uranyl bipyramids because their size is consistent with bidentate coordination of the uranyl ion by either group, and the bonding requirements of the O atoms of these groups are well-suited to form bonds to the uranyl cation. As methylenediphosphonate is more stable than pyrophosphate, the use of these two units may result in different cluster stabilities. We note that several studies have reported polyoxometalate clusters that contain pyrophosphate,[10] but no clusters or coordination compounds containing actinides and pyrophosphate have been reported.

Experimental Methods

Uranyl peroxo pyrophosphate clusters self-assemble in aqueous solution over a wide range of solution pH under ambient conditions. **Caution:** *Although the depleted uranium used in this study has a very long half-life, precautions for working with radioactive materials should be followed.* All syntheses were conducted in 5 mL glass vials, and aqueous solutions were created using ultrapure water. In all cases 0.1 mL of an aqueous 0.5 M $UO_2(NO_3)_2$ solution, 0.1 mL of 30% H_2O_2 solution, and 0.1 mL of an aqueous 2.4 M LiOH solution were combined in the vial. Pyrophosphate or methylenediphosphonate were added as solutions of either $CH_2(PO_3H_2)_2$, $Na_4P_2O_7$, or $K_4P_2O_7$. Solutions of $CH_3OHC(PO_3H_2)_2$, $N(CH_2-COOH)_3$, HOOC−COOH, NaCl, or HOOC−CH=CH−COOH were added to the aqueous solutions to promote crystallization. In all cases the synthesis of specific clusters was found to be readily repeatable, and most clusters formed in solutions exhibiting a range of pH. The details of the syntheses that resulted in the crystals studied are provided in Table 1, including the solution pH and volumes of solutions added to the reactions. The pH range under which identical clusters were crystallized is given for each cluster.

Crystals were harvested from their mother solutions as soon as they had grown large enough for single-crystal X-ray diffraction studies. The yield of clusters in solution, relative to the U and P present in solution, is unknown because solutions were not evaporated to dryness (which would have destroyed the air-sensitive crystals). However, in each case precipitates containing U or P other than the cluster-bearing crystals were absent. Small-angle X-ray scattering data (see below) readily demonstrated the presence of cage clusters in solution, which indicates a relatively high yield.

The role of the crystals in this study is to provide an ordered array of clusters suitable for X-ray diffraction analysis of the structure of the cluster. Diffraction-based studies of U-bearing clusters are challenging because of the large scattering contrast between U and the lighter elements present and because of the presence of relatively large volumes with little electron density as compared to the clusters. Furthermore, the counterions and H_2O in the intercluster regions tend to be disordered. An outcome of these structural characteristics is that many reflections are weak, and poor diffraction at higher angles limits the resolution. Previous studies have shown that details of the structural connectivities of the uranyl-based clusters are attainable through X-ray diffraction.[3,5−8,11] Intercluster atoms are usually not located, the data do not support determination of H atom positions or refinement of anisotropic displacement parameters for most O atoms, and refined U−O and P−O bond lengths have uncertainties of ∼0.02−0.04 Å.

Crystals were isolated from their mother solutions, placed on cryoloops in oil, and cooled to 110 K for data collections using a Bruker APEX diffractometer equipped with monochromated Mo Kα X-radiation. A complete sphere of data was collected for each crystal using framewidths of 0.3° in ω. Data were corrected for Lorentz, polarization, and background effects using the Bruker APEX II software, and empirical corrections for absorption were performed using SADABS. Structure solutions and refinements were done with SHELXTL.[12] Initial structure models revealed significant void spaces in each structure that contained disordered solvent molecules and counterions. Following development of a model structure for the cluster in each case, the data were corrected for solvent-accessible void space using SQUEEZE as implemented in PLATON.[13] Final refinements included anisotopic displacement parameters for U and P atoms, and either anisotropic or isotropic displacement parameters (as the data permitted) for the O, C, and counterion atoms. Crystallographic parameters are provided in the Supporting Information. The composition of each cluster as derived from the crystallographic data is given in Table 2.

(10) Dolbecq, A.; Lisnard, L.; Mialane, P.; Marrot, J.; Benard, M.; Rohmer, M. M.; Secheresse, F. *Inorg. Chem.* **2006**, *45*, 5898. du Peloux, C.; Mialane, P.; Dolbecq, A.; Marrot, J.; Secheresse, F. *Angew. Chem., Int. Ed.* **2002**, *41*, 2808. Himeno, S.; Katsuta, T.; Takamoto, M.; Hashimoto, M. *Bull. Chem. Soc. Jpn.* **2006**, *79*, 100. Kortz, U. *Inorg. Chem.* **2000**, *39*, 623.

(11) Unruh, D. K.; Burtner, A.; Pressprich, L.; Sigmon, G. E.; Burns, P. C. *Dalton Trans.* **2010**, *39*, 5807–5814.

(12) Sheldrick, G. M. *SHELXTL;* Bruker AXS, Inc.: Madison, WI, 1996.

(13) Spek, A. L. *J. Appl. Crystallogr.* **2003**, *36*, 7.

Table 2. Cluster Designations and Compositions

designation	composition
$U_{18}Py_2PCP_6$	$[(UO_2)_{18}(O_2)_{18}(OH)_2(CH_2P_2O_6)_6(P_2O_7)_2]^{34-}$
$U_{20}Py_{10}$	$[(UO_2)_{20}(O_2)_{20}(P_2O_7)_{10}]^{40-}$
$U_{20}Py_{6a}$	$[(UO_2)_{20}(O_2)_{24}(P_2O_7)_6]^{32-}$
$U_{20}Py_{6b}$	$[(UO_2)_{20}(O_2)_{24}(P_2O_7)_6]^{32-}$
$U_{24}Py_{12}$	$[(UO_2)_{24}(O_2)_{24}(P_2O_7)_{12}]^{48-}$
$U_{24}PCP_{12}$	$[(UO_2)_{24}(O_2)_{24}(CH_2P_2O_6)_{12}]^{48-}$
$U_{26}Py_6$	$[(UO_2)_{26}(O_2)_{33}(P_2O_7)_6]^{38-}$
$U_{26}Py_{11}$	$[(UO_2)_{26}(O_2)_{28}(P_2O_7)_{11}]^{48-}$
$U_{32}Py_{16}$	$[(UO_2)_{32}(O_2)_{32}(P_2O_7)_{16}]^{64-}$

Small-angle X-ray scattering (SAXS) data were collected for solutions using a Bruker Nanostar instrument equipped with a Cu microfocus source, Montel multilayer optics, and HI-STAR multiwire detector. Data were collected with a sample-to-detector distance of ~25.5 cm with the sample chamber under vacuum. Solutions were placed in 0.5 mm diameter glass capillaries with the ends of the capillary sealed using wax. Ultrapure water was placed in an identical capillary for background measurement. The sample data were corrected by background subtraction and were integrated over the 2θ range 1.0−11.0°.

Infrared spectra (see Supporting Information) were collected for crystals containing uranyl peroxide pyrophosphate clusters using a SensIR spectrometer and a diamond ATR objective.

Results

The reaction of pyrophosphate or methylenediphosphonate with uranyl nitrate gave eight topologically distinct clusters containing between 18 and 32 uranyl polyhedra as well as from 6−16 pyrophosphate (or methylenediphosphonate) units. The clusters are hereafter designated U_nPy_m, where *n* and *m* are integers giving the number of U atoms and pyrophosphate groups present in the cluster, respectively. Clusters are further distinguished by a letter designation where necessary, and PCP is substituted for Py where methylenediphosphonate is present. Cluster designations and compositions are given in Table 2.

The U^{6+} cations in all eight clusters are present as the typical $(UO_2)^{2+}$ uranyl ion, with U−O bond lengths of ~1.8 Å and O−U−O bond angles of ~180°. The uranyl ions are coordinated by ligands arranged at the equatorial vertexes of hexagonal bipyramids in which the apexes are defined by the O atoms of the uranyl ion. Each polyhedron contains two bidentate peroxide groups arranged at *cis* equatorial edges of the bipyramid. In all clusters the uranyl hexagonal bipyramids share all edges defined by either peroxide or two OH groups with other uranyl polyhedra. Completion of the bipyramidal coordination about the uranyl ions occurs in one of four ways: (1) Attachment of a pyrophosphate (or methylenediphosphonate) unit to a uranyl ion completes its coordination sphere, with an O atom from each of the two phosphate (or phosphonate) groups coordinating the uranyl ion, forming an equatorial edge of the bipyramid. (2) Two OH groups coordinate the uranyl ion and define an equatorial edge. (3) A third peroxide group coordinates the uranyl ion. (4) Two pyrophosphate units attach to the uranyl ion, with an O atom from each completing the coordination environment about the uranyl ion.

Pyrophosphate (or methylenediphosphonate) groups play an integral role in the connectivities of the clusters. All clusters contain such groups that bridge between two uranyl hexagonal bipyramids, as illustrated in Figure 1a,b. In addition to this mode of connectivity, the clusters $U_{18}Py_2PCP_6$ and $U_{26}Py_{11}$ also contain pyrophosphate groups that bridge between three uranyl hexagonal bipyramids, as shown in Figure 1c,d. This is achieved by sharing two vertexes with one hexagonal bipyramid, and one each with two other bipyramids.

$U_{24}Py_{12}$ and $U_{32}Py_{16}$. Consider first the topologically related $U_{24}Py_{12}$ and $U_{32}Py_{16}$ clusters (Figure 2). Uranyl bipyramids in these clusters share edges defined by peroxide with two adjacent bipyramids, giving a ring consisting of four such bipyramids. In $U_{24}Py_{12}$, with composition $[(UO_2)_{24}(O_2)_{24}(P_2O_7)_{12}]^{48-}$, there are six of these four-membered rings, giving a total of 24 bipyramids in the cluster (Figure 2a,b). Within the four-membered rings of bipyramids, uranyl ions are arranged such that lines parallel to them intersect below the ring. This is due to the strongly bent U−(O_2)−U dihedral angles. In the cases of four of the four-membered rings, lines parallel to the uranyl ions intersect within the cluster, and the U−(O_2)−U dihedral angles range from 130.7 to 137.1°. The sense of curvature is the opposite for the other two four-membered rings, with lines parallel to the uranyl ions intersecting outside the cluster. In these cases the U−(O_2)−U dihedral angles range from 138.3 to 142.9°, somewhat larger than those of the other four-membered rings.

The $U_{24}Py_{12}$ cluster is derived from the simpler U_{24} cluster[3] by replacing the shared OH−OH edges in the latter with pyrophosphate or methylenediphosphonate groups ($U_{24}PCP_{12}$ is isostructural with $U_{24}Py_{12}$). The OH−OH edges of the U_{24} cluster are indicated by arrows in Figure 3.

The $U_{32}Py_{16}$ cluster, with composition $[(UO_2)_{32}(O_2)_{32}(P_2O_7)_{16}]^{64-}$, is the largest reported in the current study, containing eight four-membered rings of peroxide-edge-sharing uranyl bipyramids, with a total of 32 uranyl bipyramids. These are connected through 16 different pyrophosphate units. Each of the four-membered rings is positioned such that lines drawn parallel to the uranyl ions intersect within the cluster. The U−(O_2)−U dihedral angles in this cluster range from 133.2 to 144.3°. The cluster is flattened, with maximum and minimum diameters of 28.2 and 18.0 Å, as measured from the edges of bounding O atoms. The cluster walls contain prominent openings, with the largest of these visible at the tops and bottoms of the cluster in Figure 2e. The free space in these openings, as measured from the edges of bounding O atoms, is 6.3 Å. Smaller openings have a free space of about 4.1 Å.

Graphs of $U_{24}Py_{12}$ and $U_{32}Py_{16}$ contain topological squares corresponding to the four-membered rings of peroxide-edge-sharing bipyramids (Figure 2c,f). These are linked through pyrophosphate or methylenediphosphonate. The graph for $U_{24}Py_{12}$ contains only squares and distorted hexagons. It is topologically identical to the graph of the U_{24} cluster that we reported earlier,[3] and the cluster is thus a topological derivative of U_{24}. The graph of $U_{32}Py_{16}$ contains squares, distorted hexagons, and two octagons and has no topological analogue in previously reported clusters of uranyl polyhedra.

$U_{18}Py_2PCP_6$. The cluster $U_{18}Py_2PCP_6$, with composition $[(UO_2)_{18}(O_2)_{18}(OH)_2(CH_2P_2O_6)_6(P_2O_7)_2]^{34-}$, contains 18 uranyl bipyramids. Eight of these are located toward the top of the cluster (as illustrated in Figure 4, shown separately in Figure 4d). Two bipyramids have two equatorial edges that correspond to peroxide groups and one that is defined by two hydroxyl groups. All three of these edges are shared with adjacent bipyramids, and the hydroxyl−hydroxyl bridge is noteworthy in that this is the only occurrence of this type of bridge in the eight clusters reported herein. Hydroxyl−hydroxyl bridges of this type are primary features of several of the cage clusters built from uranyl bipyramids that we reported earlier.[3,5−8,11] Each of the other bipyramids at the top of the cluster is linked to two others by sharing edges consisting of peroxide. The result is two five-membered rings of biyramids that share two bipyramids (Figure 4d).

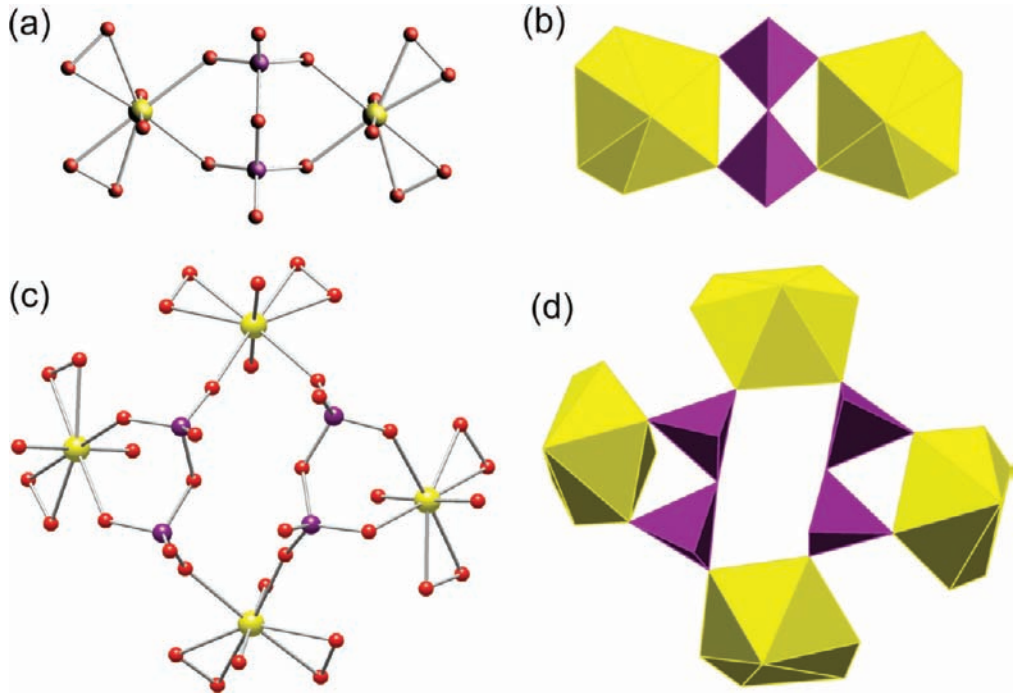

Figure 1. Linkages between uranyl bipyramids and pyrophosphate groups found in cage clusters. U atoms and polyhedra are shown in yellow, pyrophosphate groups and P atoms are colored blue-violet, and O atoms are shown as red spheres.

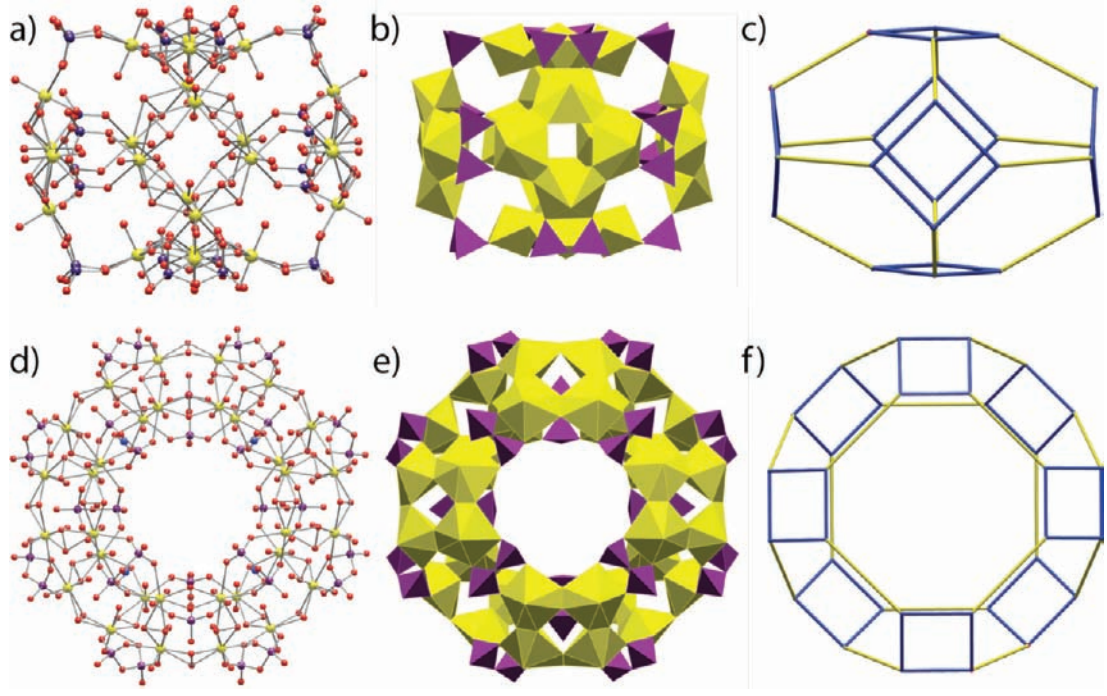

Figure 2. Uranyl peroxide pyrophosphate cage clusters $U_{24}Py_{12}$ and $U_{32}Py_{16}$ (compositions given in Table 2). For each cluster the ball-and-stick, polyhedral, and graphical representations are shown. Uranyl polyhedra and pyrophosphate tetrahedra are colored yellow and blue-violet, respectively. U, O, and P atoms are colored yellow, red, and blue-violet, respectively. Vertices in the graphs represent U atoms, and blue and yellow lines correspond to shared edges between bipyramids and bridging pyrophosphate, respectively.

Ten uranyl hexagonal bipyramids are located on the bottom of cluster $U_{18}Py_2PCP_6$ (Figure 4e). Each shares an edge defined by peroxide with two adjacent bipyramids, resulting in a 10-membered ring. Two pyrophosphate groups occur in the central regions of this ring, where they each bridge between three bipyramids.

Linkages between the top and bottom portions of cluster $U_{18}Py_2PCP_6$ are through six methylenediphosphonate groups. Each bridges between two bipyramids with the connectivity shown in Figure 1b. The graph of $U_{18}Py_2PCP_6$ exhibits a pair of pentagons that share an edge on the top and the complex 10-membered ring on the bottom (Figure 4c).

$U_{20}Py_{10}$, $U_{20}Py_{6a}$, and $U_{20}Py_{6b}$. Illustrations of the clusters $U_{20}Py_{10}$, $U_{20}Py_{6a}$, and $U_{20}Py_{6b}$, each of which contains 20 uranyl hexagonal bipyramids, are given in Figure 5. Consider first cluster $U_{20}Py_{6b}$ (Figure 5a−e), with the composition

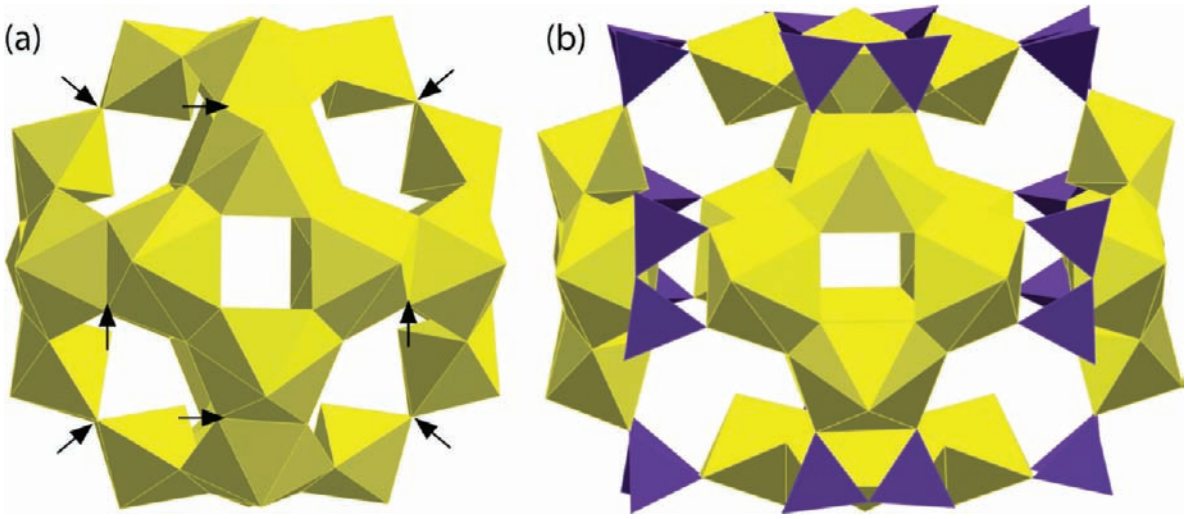

Figure 3. Polyhedral representations of the cage clusters U_{24} and $U_{24}Py_{12}$, with arrows designating OH−OH edges in U_{24} that are replaced by pyrophosphate units in $U_{24}Py_{12}$. Legend as in Figure 2.

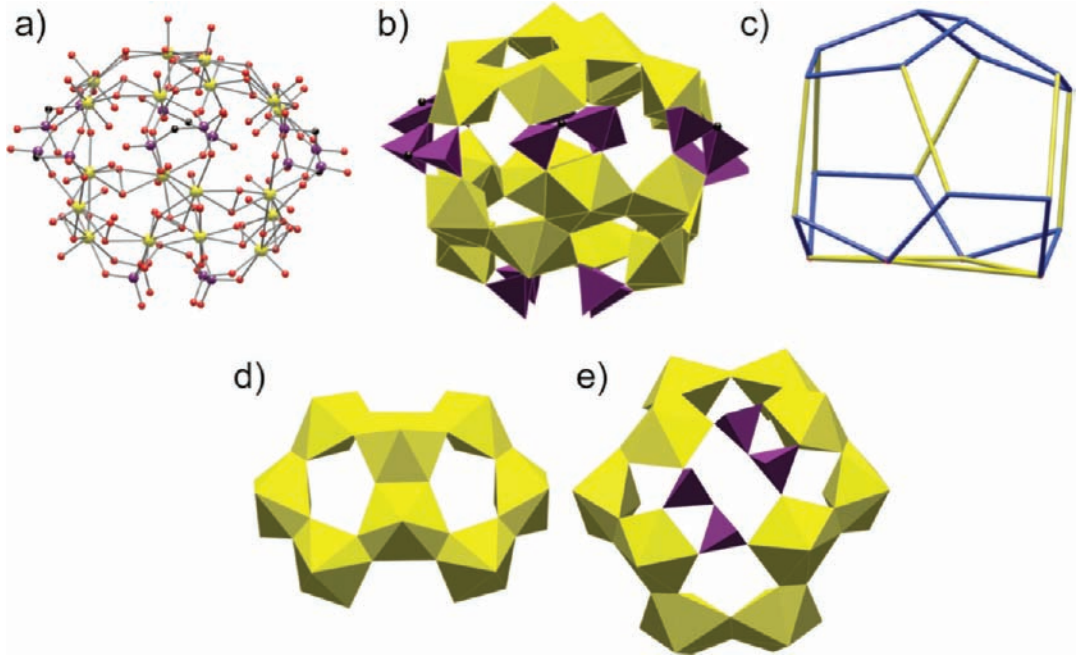

Figure 4. Uranyl peroxide pyrophosphate cage cluster $U_{18}Py_2PCP_6$ (composition given in Table 2). Legend as in Figure 2, except that C atoms are shown as black spheres.

$[(UO_2)_{20}(O_2)_{24}(P_2O_7)_6]^{32-}$. It contains two distinct components that consist of uranyl bipyramids. One of these, located at the top of the cluster, contains eight bipyramids (Figure 5d). Two of these have three equatorial edges that are defined by peroxide groups, and they share one of these edges. The remaining six bipyramids each contain two peroxide groups that are located at edges that are shared within five-membered rings of bipyramids that have two polyhedra in common. The bottom of the cluster consists of 12 uranyl hexagonal bipyramids (Figure 5e). In six of these bipyramids, three of the equatorial edges correspond to peroxide groups, and in each case all of these edges are shared with adjacent polyhedra. Only two edges of the bipyramids correspond to peroxide groups in the other six bipyramids, and again each of the peroxide edges is shared with other bipyramids. The result is four five-membered rings of bipyramids that are fused through common bipyramids. Linkages between the uranyl polyhedral building units are through six pyrophosphate groups with the configuration shown in Figure 1b. The graph of the cluster $U_{20}Py_{6b}$ contains a dimer of pentagons on top and the tetramer of pentagons on bottom.

The cluster $U_{20}Py_{6a}$, with composition $[(UO_2)_{20}(O_2)_{24}(P_2O_7)_6]^{32-}$, contains two uranyl polyhedral units that are related through an inversion center (Figure 5f−i). Each contains 10 uranyl bipyramids (Figure 5i). Four of these contain three peroxide groups that are located along equatorial edges, with these edges shared with three adjacent bipyramids. Two edges are defined by peroxide groups in six bipyramids, and the corresponding edges are also shared with adjacent bipyramids. Six pyrophosphate groups link the two uranyl bipyramid units into the cage cluster, with the connectivity illustrated in Figure 1b. The corresponding graph exhibits two trimers of edge-sharing pentagons, each of which corresponds to 10 peroxide-edge-sharing bipyramids (Figure 5h). Linkage through the pyrophosphate groups generates additional topological pentagons.

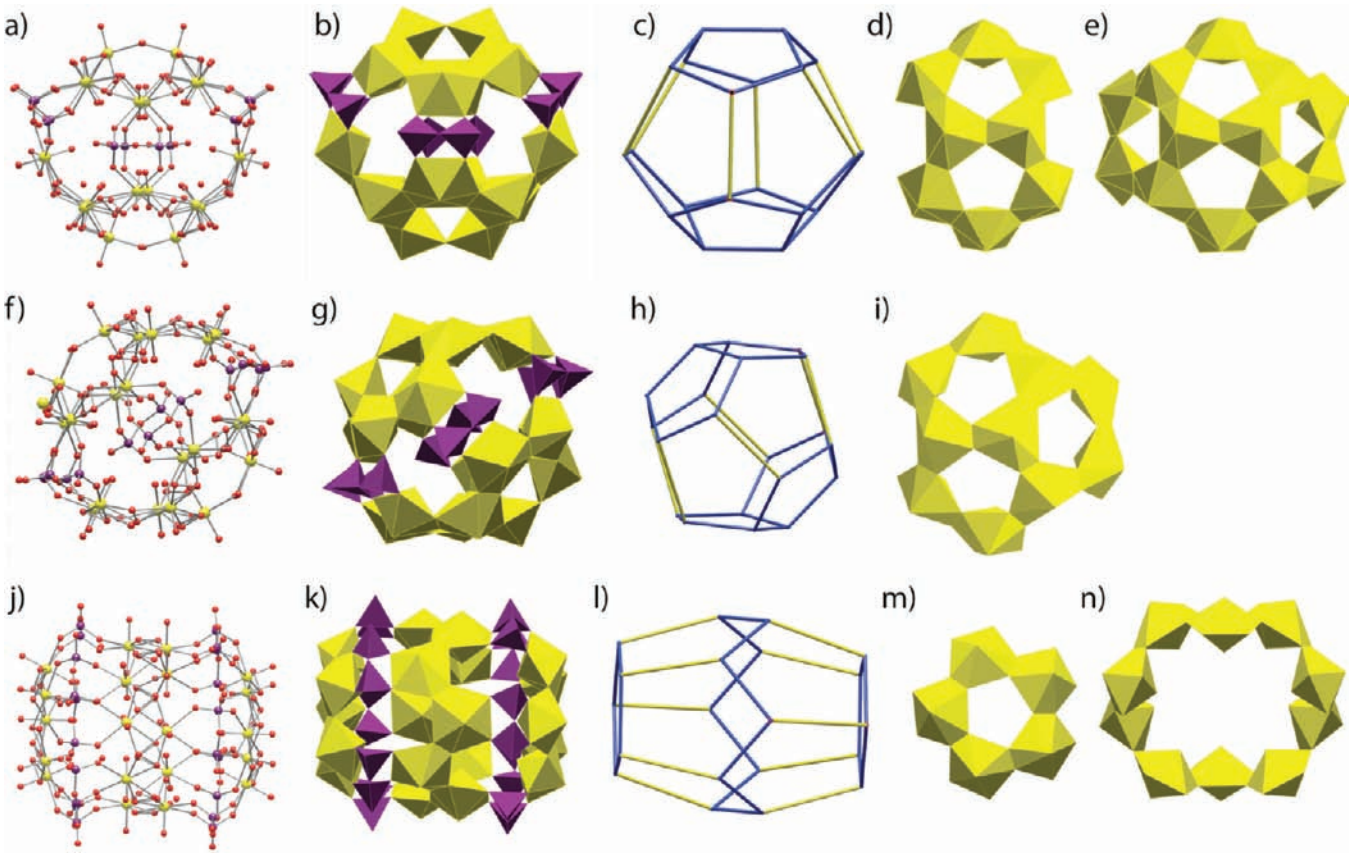

Figure 5. Uranyl peroxide pyrophosphate cage clusters $U_{20}Py_{10}$, $U_{20}Py_{6a}$, and $U_{20}Py_{6b}$ (compositions given in Table 2). Legend as in Figure 2.

Whereas the $U_{20}Py_{6a}$ and $U_{20}Py_{6b}$ clusters are topologically closely related and chemically identical, the cage cluster $U_{20}Py_{10}$ is distinct (Figures 5j−n). The cluster, with composition $[(UO_2)_{20}(O_2)_{20}(P_2O_7)_{10}]^{40-}$, is truncated on the left and right sides by rings that consist of five uranyl bipyramids. Each of these contains two peroxide edges that are shared with adjacent bipyramids, giving a five-membered ring (Figure 5m). The central region of the cluster contains 10 uranyl bipyramids, each of which contains two peroxide edges that are shared with adjacent bipyramids. The result is a 10-membered ring (Figure 6n). Ten pyrophosphate groups link these three uranyl bipyramidal units into a closed cluster, with the mode of this linkage shown in Figure 1b. The graph of $U_{20}Py_{10}$ shows the pentagons at either end that represent five-membered rings of peroxide-edge-sharing hexagonal bipyramids as well as the complex 10-membered ring of peroxide-edge-sharing bipyramids (Figure 5l). Note that linkage through the pyrophosphate units gives rise to topological pentagons.

Considering the graphs of the cage clusters $U_{20}Py_{10}$, $U_{20}Py_{6a}$, and $U_{20}Py_{6b}$ (Figure 5c,h,l), it is apparent that each consists of 12 pentagons, although some of the pentagons are significantly distorted. Ignoring the distortions of the pentagons, all have identical topologies. Furthermore, their topologies are the same as found for U_{20} previously,[7] and thus these three clusters are derivatives of the U_{20} cluster that contains only uranyl hexagonal bipyramids (Figure 6). The topology of all four of these clusters consists of 12 pentagons only, with 20 vertexes, and is the smallest possible fullerene topology.

$U_{26}Py_{11}$ and $U_{26}Py_6$. The $U_{26}Py_{11}$ and $U_{26}Py_6$ cage clusters, with compositions $[(UO_2)_{26}(O_2)_{28}(P_2O_7)_{11}]^{48-}$ and $[(UO_2)_{26}(O_2)_{33}(P_2O_7)_6]^{38-}$, respectively, both contain 26 uranyl hexagonal bipyramids (Figure 7). The top portion of $U_{26}Py_{11}$ (relative to the orientation in Figure 7) is shown in Figure 7d. It consists of 16 uranyl bipyramids. Four of these have three equatorial edges defined by peroxide groups, whereas each of the other 12 contain only two peroxide groups. In all cases equatorial edges of bipyramids that are peroxide are shared between two bipyramids. There are two five-membered rings of edge-sharing bipyramids in this structural unit, and these are connected through six additional bipyramids to create an open ring. Two pyrophosphate groups occur within this ring, where each of them bridges between three bipyramids with the connectivity shown in Figure 1d. The bottom of the $U_{26}Py_{11}$ cage cluster contains 10 uranyl hexagonal bipyramids, each of which has two equatorial edges that correspond to peroxide. All peroxide groups are shared between two bipyramids, giving two five-membered rings of bipyramids (Figure 7e). These rings are linked through one pyrophosphate group with the connectivity shown in Figure 1b. Eight pyrophosphate groups link the bottom and top portions of the cluster, each with the configuration shown in Figure 1b. The graph of $U_{26}Py_{11}$ shows two isolated pentagons on the bottom and the 16-membered ring of peroxide-edge-sharing bipyramids on the top (Figure 7c).

The cluster $U_{26}Py_6$ contains 26 uranyl hexagonal bipyramids, 14 of which have three equatorial edges that are defined by peroxide. The remaining 12 bipyramids all have two peroxide equatorial edges (Figure 7f−j). All peroxide groups are shared between two bipyramids; thus, 14 bipyramids are linked to three other bipyramids, and 12 share edges with only two. The uranyl polyhedral portion of the cluster is shown in two orientations in Figure 7i,j, and it contains eight five-membered rings of bipyramids that are linked into a

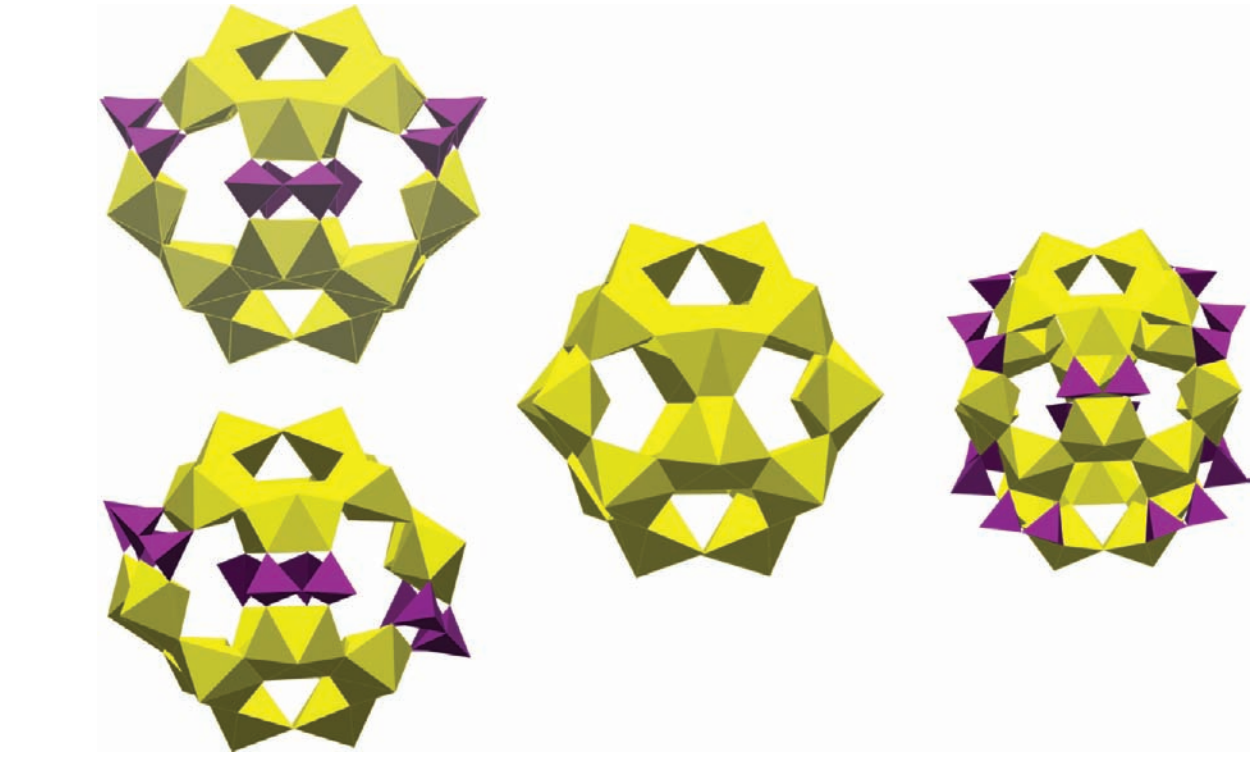

Figure 6. Uranyl peroxide pyrophosphate cage clusters $U_{20}Py_{10}$ (right), $U_{20}Py_{6a}$ (bottom left), and $U_{20}Py_{6b}$ (top left) compared to the U_{20} cluster in the center. Legend as in Figure 2.

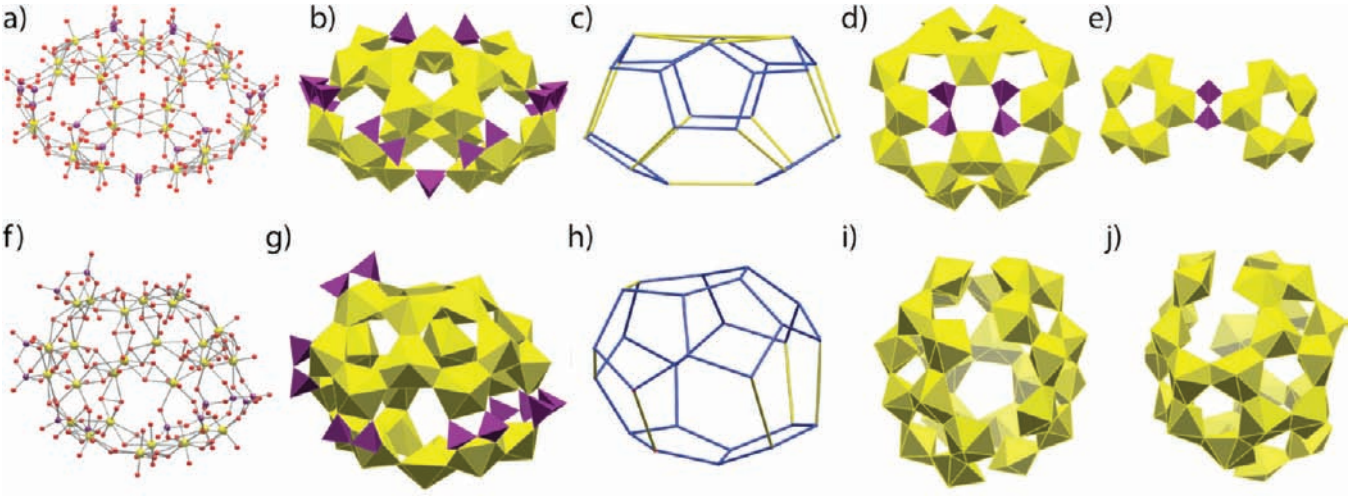

Figure 7. Uranyl peroxide pyrophosphate cage clusters $U_{26}Py_{11}$ and $U_{26}Py_6$ (compositions given in Table 2). Legend as in Figure 2.

chain. This is more apparent in the graph of $U_{26}Py_6$, which shows that the eight edge-sharing pentagons form a chain that extends over much of its circumference (Figure 7h). Six pyrophosphate groups provide linkages between different bipyramids within the uranyl bipyramid chain, each with the connectivity shown in Figure 1b.

SAXS Study. Small-angle X-ray scattering (SAXS) data collected for ultrapure water in which harvested crystals of $U_{26}Py_6$ or $U_{32}Py_{16}$ had been dissolved indicated clusters were present in solution (see Supporting Information). The scattering curves were fit using a spherical model ($U_{26}Py_6$) or spherical-shell model ($U_{32}Py_{16}$) that gave a radius of 10.1 Å for the $U_{26}Py_6$ cluster and 5.4 (inner) and 10.5 Å for the $U_{32}Py_{16}$ cluster. The crystallographically derived structures of these clusters gave outer radii, measured from the centers of bounding O atoms, ranging from 8.5 to 10.5 Å for $U_{26}Py_6$ and from 7.2 to 12.2 Å for $U_{32}Py_{16}$. The SAXS data are consistent with $U_{26}Py_6$ or $U_{32}Py_{16}$ clusters persisting upon dissolution in ultrapure water.

SAXS data were also collected for aliquots of parent solutions that were in contact with crystals minutes earlier. Solutions over crystals of $U_{20}Py_{10}$ and $U_{24}Py_{12}$ provided scattering profiles that could readily be fit using monodisperse spherical models with radii 5.9 and 9.0 Å, respectively. SAXS data collected for parent solutions of $U_{20}Py_{6a}$, $U_{20}Py_{6b}$, $U_{26}Py_6$, and $U_{32}Py_{16}$ all indicated polydispersity, although in all cases the scattering was consistent with clusters of dimensions similar to those found in the

crystallographic studies. The growing crystals likely select specific clusters from a polydisperse solution in at least some cases.

Discussion

To date, our research group has reported the synthesis and structures of 13 cage clusters built from only uranyl bipyramids,[3,5−7,11] three open clusters of uranyl hexagonal bipyramids,[8] two organic−inorganic clusters consisting of oxalate groups and uranyl hexagonal bipyramids,[14] and the eight cage clusters reported herein that consist of pyrophosphate or methylenediphosphonate groups and uranyl bipyramids. These discoveries were realized from a sustained combinatorial synthesis program using U, as there is no suitable nonradioactive analogue for the higher-valence actinide cations. This rapidly growing family of clusters requires no template for assembly, relying only on the curvature inherent in the U−(O_2)−U bridge to stimulate formation.[7] With the addition of the uranyl pyrophosphate clusters, we have demonstrated that uranyl-based clusters can be formed in aqueous solutions with pH values in the range of 4−13. We also demonstrated that some of these clusters remain intact after dissolution in ultrapure water, even in cases where the initial synthesis conditions were alkaline.

A variety of applications of uranyl (or actinyl in general) cage clusters could emerge in an advanced nuclear energy system, for control of chemical composition in fuel fabrication, for development of a "greener" reprocessing cycle, or as precursor materials for the synthesis of novel waste forms for radionuclides that cannot be recycled. We are particularly interested in how topological and compositional details of uranyl-based cage clusters will impact their properties and potential applications, and we are addressing these issues in ongoing studies.

We have shown that some of the uranyl pyrophosphate cage clusters introduced here are topologically identical to the simpler clusters that contain only uranyl hexagonal bipyramids (specifically the $U_{24}Py_{12}$, $U_{20}Py_{10}$, $U_{20}Py_{6a}$, and $U_{20}Py_{6b}$ clusters), but those of $U_{32}Py_{16}$, $U_{18}Py_2PCP_6$, $U_{26}Py_{11}$, and $U_{26}Py_6$ all present new topologies. Thus, in comparison to clusters containing only uranyl hexagonal bipyramids, introduction of pyrophosphate results in new topologies as well as larger clusters for a given number of uranyl bipyramids. Insertion of pyrophosphate also provides for very different pore sizes relative to clusters containing only uranyl bipyramids, as demonstrated by the $U_{32}Py_{16}$ cluster in particular. Creating more chemically complex clusters by incorporating units such as pyrophosphate or methylenediphosphonate should foster differences in surface properties, radius-to-charge ratios, and thus also aqueous solubility.

Some of the SAXS data collected for solutions containing uranyl pyrophosphate clusters indicated polydispersity. There is considerable uncertainty concerning the role of multiple cluster topologies and compositions in solution in our synthesis, which precludes detailed analysis of relationships between topology and solution parameters. The least soluble cluster to form is likely to be the one that crystallizes. Relative to the clusters we have isolated and studied in crystals, the important factors appear to be the pH of the mother solution and the U:P ratio. Clusters formed in solutions ranging from pH 4.0 to 11.5, although specific clusters crystallized under a much more limited pH range. Clusters containing topological squares seem to be favored by the use of Na as a counterion, whereas K tends to result in topological pentagons. This is presumably due to steric constrains concerning linkages between the O atoms of uranyl ions and these cations, with larger cations encouraging larger rings of uranyl hexagonal bipyramids.

Acknowledgment. This research was supported by the Materials Science of Actinides Center, an Energy Frontier Research Center funded by the U.S. Department of Energy, Office of Science, Office of Basic Energy Sciences, under Award Number DE-SC0001089. ICP-OES analyses were done in the Center for Environmental Science and Technology at the University of Notre Dame.

Supporting Information Available: Crystallographic data (CIF) for all compounds, infrared spectra, and small-angle X-ray scattering data. This material is available free of charge via the Internet at http://pubs.acs.org.

JA1048219

(14) Ling, J.; Wallace, C. W.; Szymanowski, J. E. S.; Burns, P. C. *Angew. Chem., Int. Ed.* **2010**, DOI: 10.1002/anie.201003197.